Supplementary Information

Brick1 is an essential regulator of actin cytoskeleton required for embryonic development and cell transformation

by B. Escobar et al…

Supplementary Methods

BRK1 expression and reporter assays. Brk1-EGFP fusion proteins were generated by subcloning the Brk1 cDNA into the pEGFP-N1 vector (Clontech). Brk1 transcripts were analyzed in a variety of mouse tissues by hybridization on RNA membranes (Zyagen) using the full mouse Brk1 cDNA was used as a probe. For detection of β-galactosidase activity in embryos and adult tissues, samples were included in OCT compound (Sakura) and frozen. X-Gal staining of 10 μm thick cryosections was performed as described (1). Counter-staining of cryostat sections was performed with nuclear fast red. Whole-mount staining of embryos or tissues was performed after fixation with glutaraldehyde and paraformaldehyde by incubating these samples with the X-Gal solution during 24 h (1). After X-Gal staining, these embryos or organs were fixed in formalin, embedded in paraffin and five- μm sections were counterstained with nuclear fast red.

Collagen degradation assays. These assays were performed essentially as described in Bravo-Cordero et al. (2). Briefly, U2OS, 786O and SN12C cells were transfected with the different constructs and 24 h after transfection, cells were plated at low density onto

2D-Collagen I-coated coverslips, and incubated for additional 24 h. After fixation, the collagen layer was immunostained using anti-Collagen I antibody (Sigma C2456) and cells were labelled using CellMask dye (C10046 from Invitrogen). As negative control for degradation we used a general MMP inhibitor (GW6001) that set up the background of the experiment. The quantification of degraded area was performed using ImageJ software.

Characterization of Brk1 Mutant Mice. For mouse genotyping, amplification of the wild-type and targeted DNA alleles was performed using an equimolecular mixture of the following oligonucleotides: Fw_int_1.5, 5'- GCGCTTTAATGTAGGGTCCA-3'; B32_Rv: 5'-CGTTACCCAACTTAATCGCCTTG-3' and Rv_int_2.1: 5'-CTGTTAAGCCTGATGACCTGAGT-3'. The sizes of the diagnostic PCR products are 500 bp and 1800 bp for the wild-type and for the targeted *Brk1* allele, respectively.

Supplementary Figures and Videos

Suppl. Figure 1. Brk1 is required for proper formation of cellular protrusions. (**A**) Wound-healing assay in PC3 cells expressing short hairpin RNAs against Brk1 (shBrk1) or scrambled sequences (Control). PC3 cells have about 80% reduction in their ability to close the area 16 h after the wound once Brk1 is downregulated. (**B**) Brk1 shows an enriched localization at membrane protrusions and lamellipodia when fused to the fluorescent protein EGFP in PC3 cells. Brk1 co-localizes with to actin, Arp2 or Wave2 at these cellular protusions as detected by immunofluorescence. A detailed observation of the EGFP signal by video microscopy confirms a dynamic re-distribution of Brk1 towards cell protrusions (Suppl. Video 5). (**C**) Brk1 down-regulation in PC3 cells results in absence of lamellipodia which are substituted by finger-like protusions.

Actin (green), but not Arp2 (upper panel) and Wave2 (bottom panel) (red) proteins are localized at the distal tips of these protusions. Blue signal indicates nuclear staining (DAPI). Bars represent 10 μm.

Suppl. Figure 2. Selection of U2OS stable clones carrying short hairpin RNAs (shRNAs) against Brk1. (**A**) U2OS cells were transfected with Brk1 shRNAs as described previously (3). The expression of Brk1 was tested by RT-PCR for multiple clones (2-6) and clone 5 was selected for most assays in U2OS. C (Control) indicates scrambled sequences. (**B**) Morphological changes in U2OS expressing shRNAs against Brk1 (clones 4 and 5). These cells remain as grouped colonies with significant changes in cellular shape as described in the main text (Suppl. Videos 3 and 4). (**C**) Colony formation assays in representative cultures expressing scrambled shRNAs (shCtrl) or shBrk1-specific shRNAs.

Suppl. Figure 3. (**A**) VHL mutation does not affect Brk1 migration implications. The VHL gene mutated ccRCC cell line 786-O behaves similarly, in a wound-healing assay, as the other cell lines tested when Brk1 is downregulated. Cells have about a 30% reduction in their motility when Brk1 is downregulated. (**B**) Brk1 silencing has no effect on ECM degradation and MMP secretion. Degradation of the extracellular matrix by U2OS or ccRCC cells was tested in the presence or absence of Brk1 shRNA. Stably transfected cells were seeded on top of a collagen layer and allowing its degradation during 24 hours. Then the collagen degraded area is measured. The MMP inhibitor GW6001 was used to set up the minimal ECM degradation background. None of the cells expressing the Brk1 shRNA show significant differences of ECM degradation

compared to the control cells. Therefore, MMP secretion and ECM degradation does not seem to be regulated by Brk1.

Suppl. Figure 4. Selection of B16F10 stable clones expressing shRNAs against Brk1. (**A**) B16F10 expressing a luciferase construct were transfected with Brk1 shRNAs as described previously (3). Brk1 downregulation was tested by wound-healing assay in all the clones (1 to 4); clone 1 was quantified showing only a 30% efficiency in recovering the wounded area. This sh1 clone was therefore selected for further assays in B16F10 cells and therefore verify by RT-PCR. (**B**) Morphological defects and lack of actin stress fibers in the B16F10 sh1 clone (shBrk1). Stress fibers (arrows) are quite evident by phalloidin staining (Actin; green) in cells treated with scrambled (shCtrl) but not in Brk1-specific shRNAs (shBrk1). Vinculin is shown in red and DNA (DAPI) in blue. Scale bar, 20 μM. (**C**) B16F10 sh1 clone were used for a metastasis assay in vivo as described in the main text. Lungs from control of shBrk1 cells were analyzed by histology (hematoxilin and eosin staining; H&E) or immunodetection of Ki67. As described in the main text, the number of melanoma nodules in mice injected with shBrk1 cells is significantly reduced versus control samples. However, the few nodules found in mice injected with shBrk1 cells display similar mitotic index (arrows in H&E insets) and Ki67 expression (brown signal in Ki67 insets), thus suggesting that these nodules have escaped from the inhibitory effect of Brk1. Unfortunately, our Brk1 antibody does not function in immunohistochemistry analysis and whether the shRNA against Brk1 is still active in these samples is not known.

Suppl. Figure 5. *Brk1* mutant alleles and Brk1 expression in embryos. **(A)** Schematic representation of the mouse chromosome 6 region containing the neighbour genes *Brk1*

and *VHL*. Both genes contain three exons including 5' and 3' unstranslated regions (white boxes). (**B**) *Brk1* mutant allele generated by an insertion of the β-geo cassette in intron 1. This insertion results in a mutant transcript driven by the endogenous *Brk1* promoter and encoding the first 42 amino acids of Brk1 and the β-*geo* gene encoding β-galactosidase and the neo-resistance gene. The position of the oligonucleotides used for PCR amplification is shown by small blue arrows. SA-β-geo-pA corresponds to the Splicing Aceptor-β-Galactosidase-neomycin resistance fusion gene-polyadelnylation site. This cassette has been inserted between positions 10,139,050-1 of mouse chromosome 6 (NCBIM37, Ensembl database). Blue nucleotides correspond to the beginning and end of the SA-γ-geo-pA cassette whereas endogenous intron sequence is shown in back. (**C**) Sequence of the oligonucleotides used for PCR amplification. (**D**) Representative PCR amplification of wild-type (+) and mutant (–) *Brk1* alleles using F5, R1 and B32.

Suppl. Figure 6. Expression of Brk1 during embryonic development. (**A**) β-galactosidase activity (blue) in E6.5 *Brk1*(+/–) embryos in 5 μm-thick cryosections. (**B**) Whole-mount analysis of E13.5 embryos showing strong and ubiquitous expression of *Brk1*-β-*geo* in *Brk1*(+/–) but not *Brk1*(+/+) embryos. Sagital sectioning of these samples indicates β-galactosidase signals in neuroepithelium (NE), heart (HR) and the wall of blood vessels (BV) (magnified squares) among other tissues. Bars: 1 mm (whole mount and whole sagital sections) or 0.1 mm (right panels). (**C**) Expression of *Brk1* transcripts as detected by in situ hybridization with a *Brk1* antisense probe. Tissues with significant levels of expression include the brain cortex and cranial and dorsal root ganglia, salivary gland and the kidney. Data from the GenePaint database **(**www.genepaint.org; Set ID:ES155**).**

Suppl. Figure 7. Brk1 expression in adult mice. **(A)** Northern blot analysis of Brk1 expression in adult mouse tissues using the full Brk1 cDNA as a probe. β-Actin was used as a control. Brain, liver and kidney are tissues were the Brk1 signal is increased when compared to α-Actin levels. (**B**) β-galactosidase activity in the indicated tissues from *Brk1*(+/+) or *Brk1*(+/–) mice. Whole-mount tissues were stained with X-Gal, embedded in parafin for better tissue conservation and sections were counterstained with nuclear fast red. Additional samples were first cryo-preserved (Cryo) and the corresponding sections were stained for β-galactosidase activity resulting in increased signal. Reporter analysis indicates high expression in hippocampus, and the brain cortex, glomerular and tubular structures in the kidney, smooth and striated muscle (both cardiac and skeletic) cells, pneumocytes type I and II (alveoli) and bronchial (Clara) cells, cartilage, intestine and red (including megakaryocytes and macrophages), but not white (lymphocytes), pulp in the spleen. Original magnification was 100X and 400X (insets).

Suppl. Figure 8. Expression of murine and human *Brk1* transcripts in different tissues and cell types from public microarray data. Data from the Genomics Institute of the Novartis Research Foundation (http://biogps.gnf.org/).

Supplementary Video 1. Renal Clear Cell Carcinoma cells (SN12C) transfected with scrambled short hairpin interfering RNA. These cells display a rapid division cycle and high motility in the plates. Cells were recorded during 16 hours with 400X magnification in a DeltaVision microscope.

Supplementary Video 2. Renal Clear Cell Carcinoma cells (SN12C) transfected with short hairpin interfering RNA against Brk1. SN12C Brk1-silenced cells divide but daughter cells remain together forming clusters and cells show a dramatic reduced motility. Cells were recorded during 16 hours with 400X magnification in a DeltaVision microscope.

Supplementary Video 3. U2OS cells transfected with scrambled short hairpin interfering RNA. These cells were detached from the plates and allowed to attach and divide at low density. These cells display a rapid division cycle and high motility in the plates. Cells were recorded during 16 hours with 400X magnification in a DeltaVision microscope.

Supplementary Video 4. U2OS cells transfected with short hairpin interfering RNA against Brk1. These cells were detached from the plates and allowed to attach and divide at low density. These Brk1-silenced cells divide but daughter cells remain together forming small clusters with reduced motility. Cells were recorded during 16 hours with 400X magnification in a DeltaVision microscope.

Supplementary Video 5. Dynamic distribution of a Brk1-GFP construct in PC3 cells showing intense cytoplasmic expression and a specific localization at the cellular protusions. The video was recorded during 10 minutes with a 63X objective and 4.5X zoom in a Leica TSC SP2 AOBS microscope using Leica Confocal Software (Leica, Mannheim, Germany)

Supplementary References

1. Hogan B, Beddington R, Costantini F, Lacy E. Manipulating the mouse embryo: A laboratory manual. Cold Spring Harbor, NY. 1994.
2. Bravo-Cordero JJ, Marrero-Diaz R, Megias D, Genis L, Garcia-Grande A, Garcia MA, et al. MT1-MMP proinvasive activity is regulated by a novel Rab8-dependent exocytic pathway. Embo J. 2007;26:1499-510.
3. Cascon A, Escobar B, Montero-Conde C, Rodriguez-Antona C, Ruiz-Llorente S, Osorio A, et al. Loss of the actin regulator HSPC300 results in clear cell renal cell carcinoma protection in Von Hippel-Lindau patients. Hum Mutat. 2007;28:613-21.

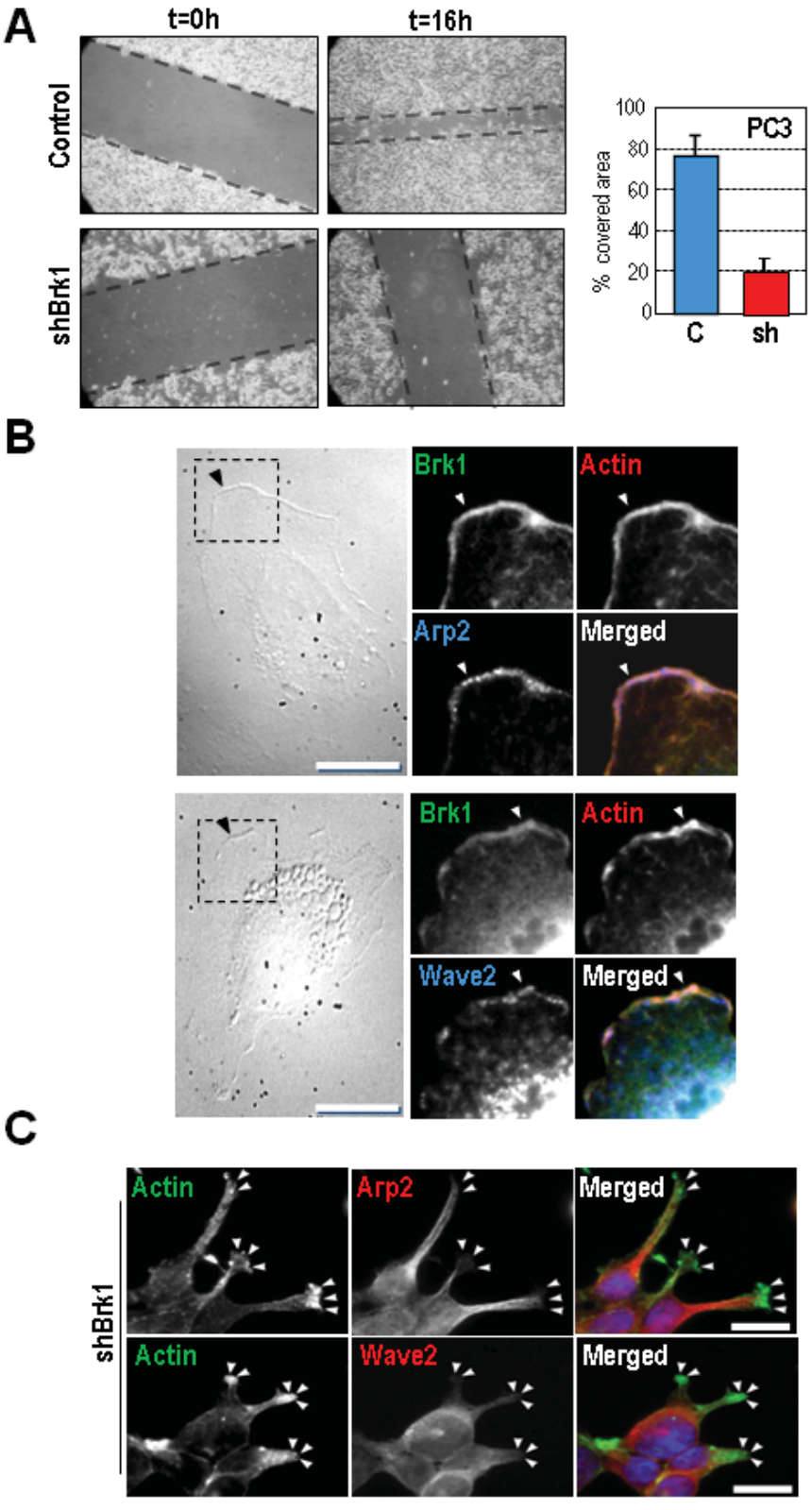

Escobar et al. Suppl. Figure 1

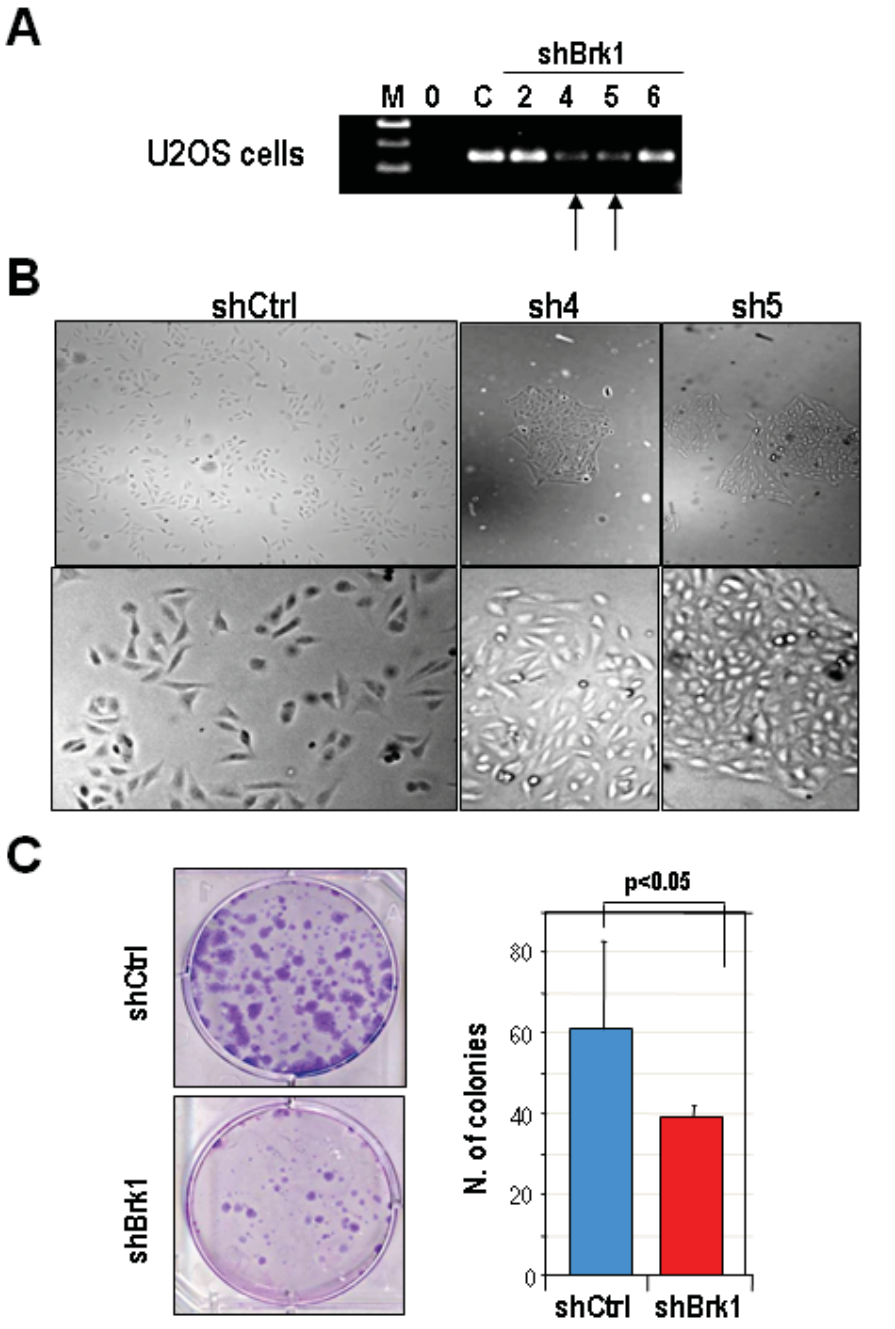

Escobar et al. Suppl. Figure 2

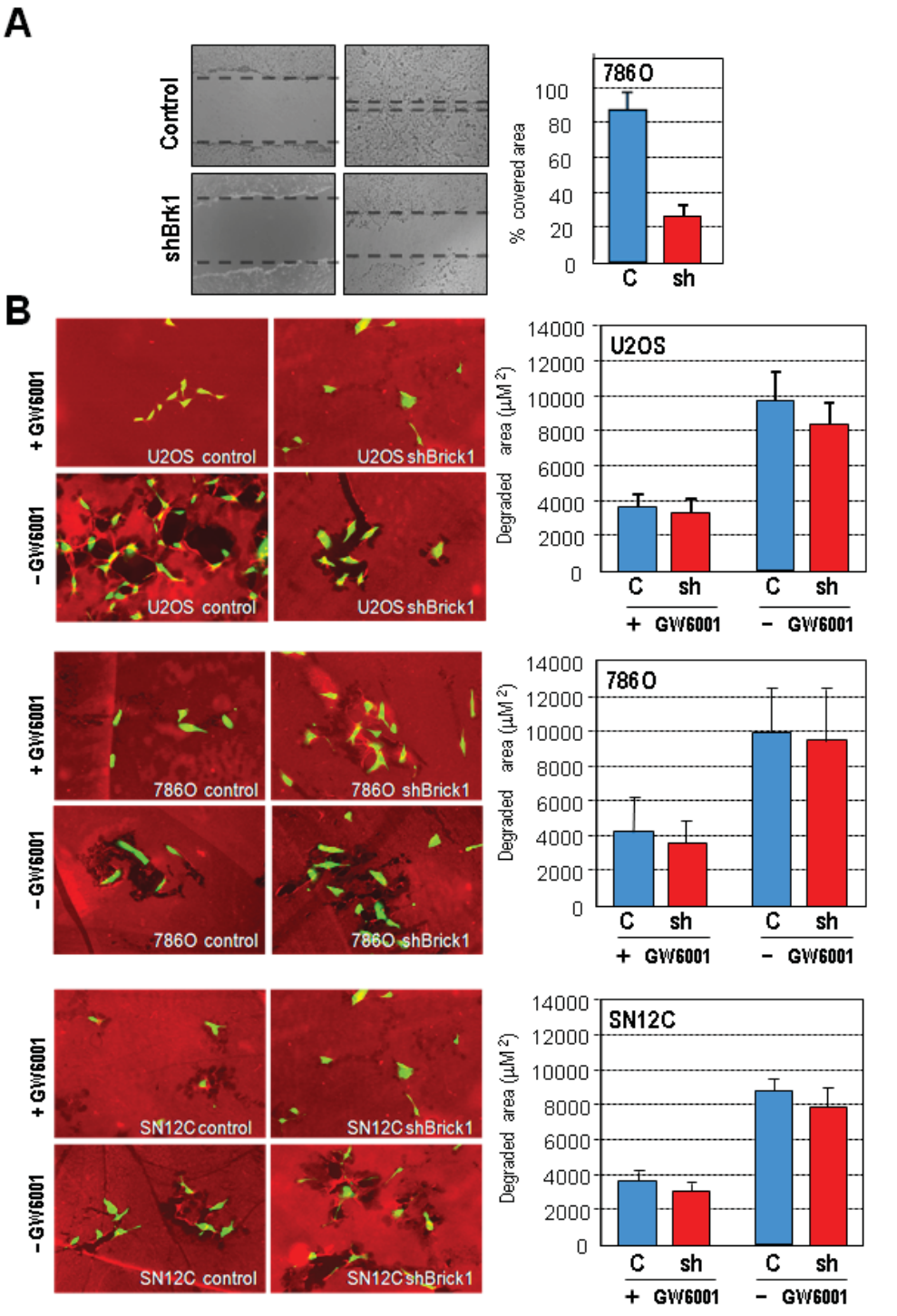

Escobar et al. Suppl. Figure 3

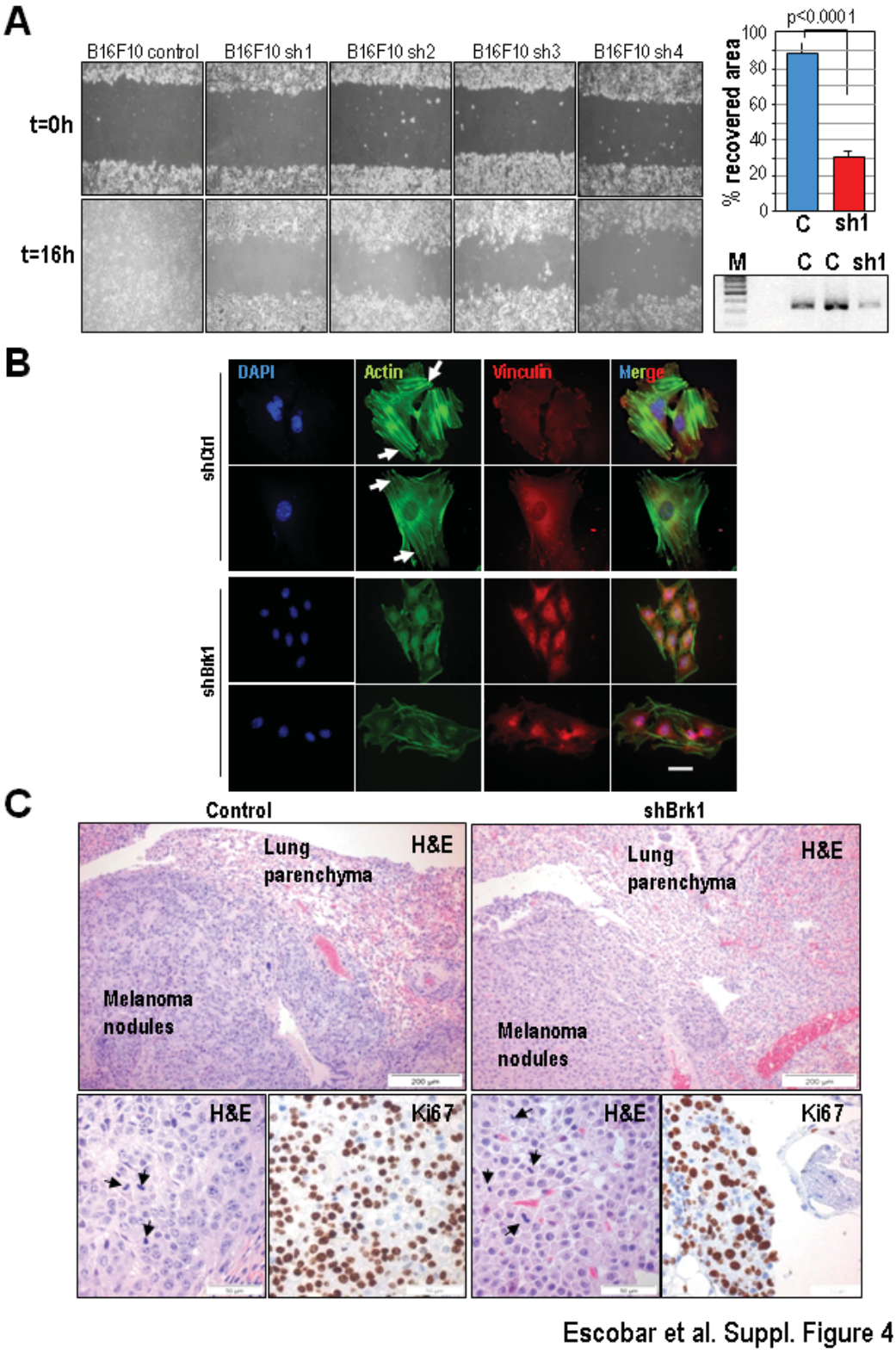

Escobar et al. Suppl. Figure 4

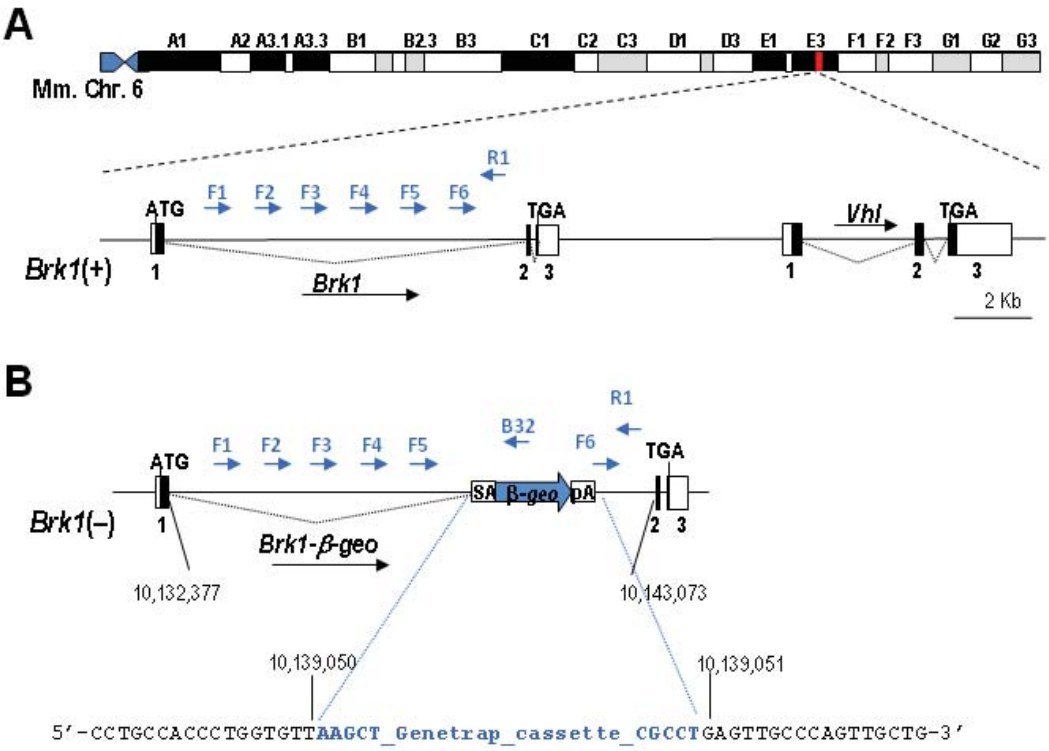

C

Primer name	Sequence
F1	5′-GAGACTCCTGCTCGTTGTCC-3′
F2	5′-GTAAAGGCCACCAACCTGAA-3′
F3	5′-TATACCTGTGAACCTACCTTGC-3′
F4	5′-TACACCATCTGACACAGCTGG-3′
F5	5′-GCGCTTTAATGTAGGGTCCA-3′
F6	5′-GCCAGAACCACAAGACCAAT-3′
R1	5′-CTGTTAAGCCTGATGACCTGAGT-3′
B32	5′-CGTTACCCAACTTAATCGCCTTG-3′

D

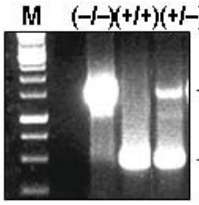

Escobar et al. Suppl. Figure 5

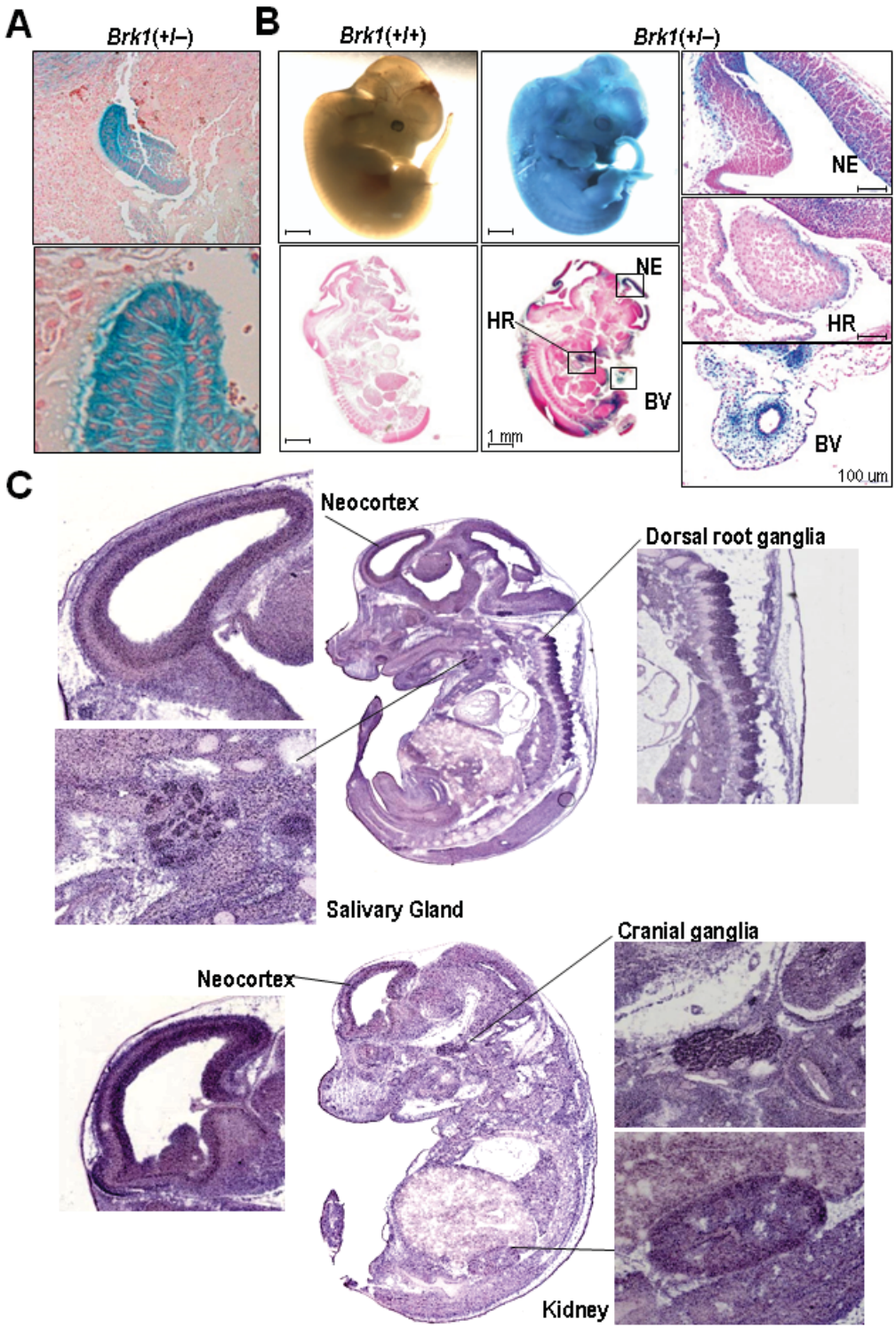

Escobar et al. Suppl. Figure 6

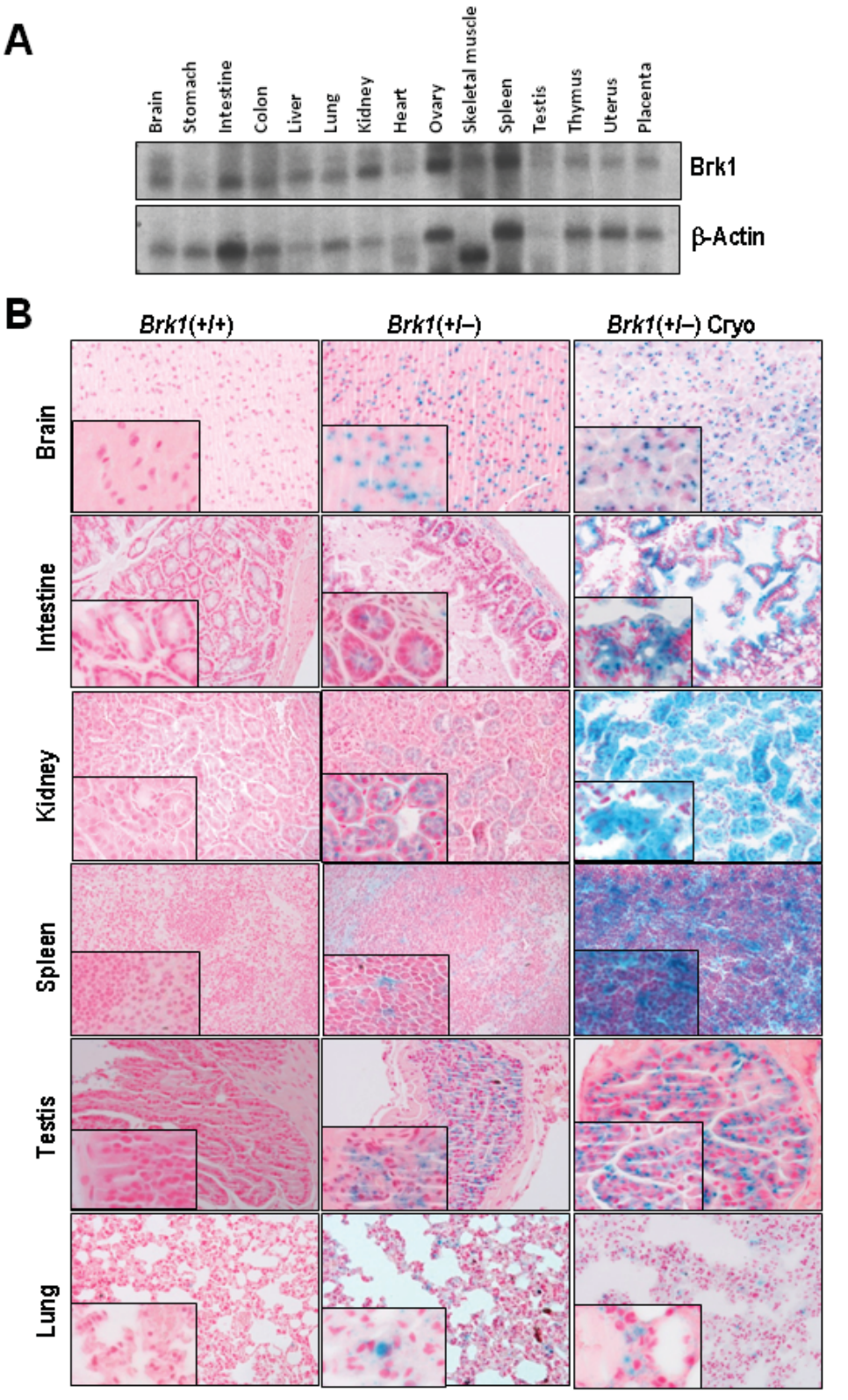

Escobar et al. Suppl. Figure 7

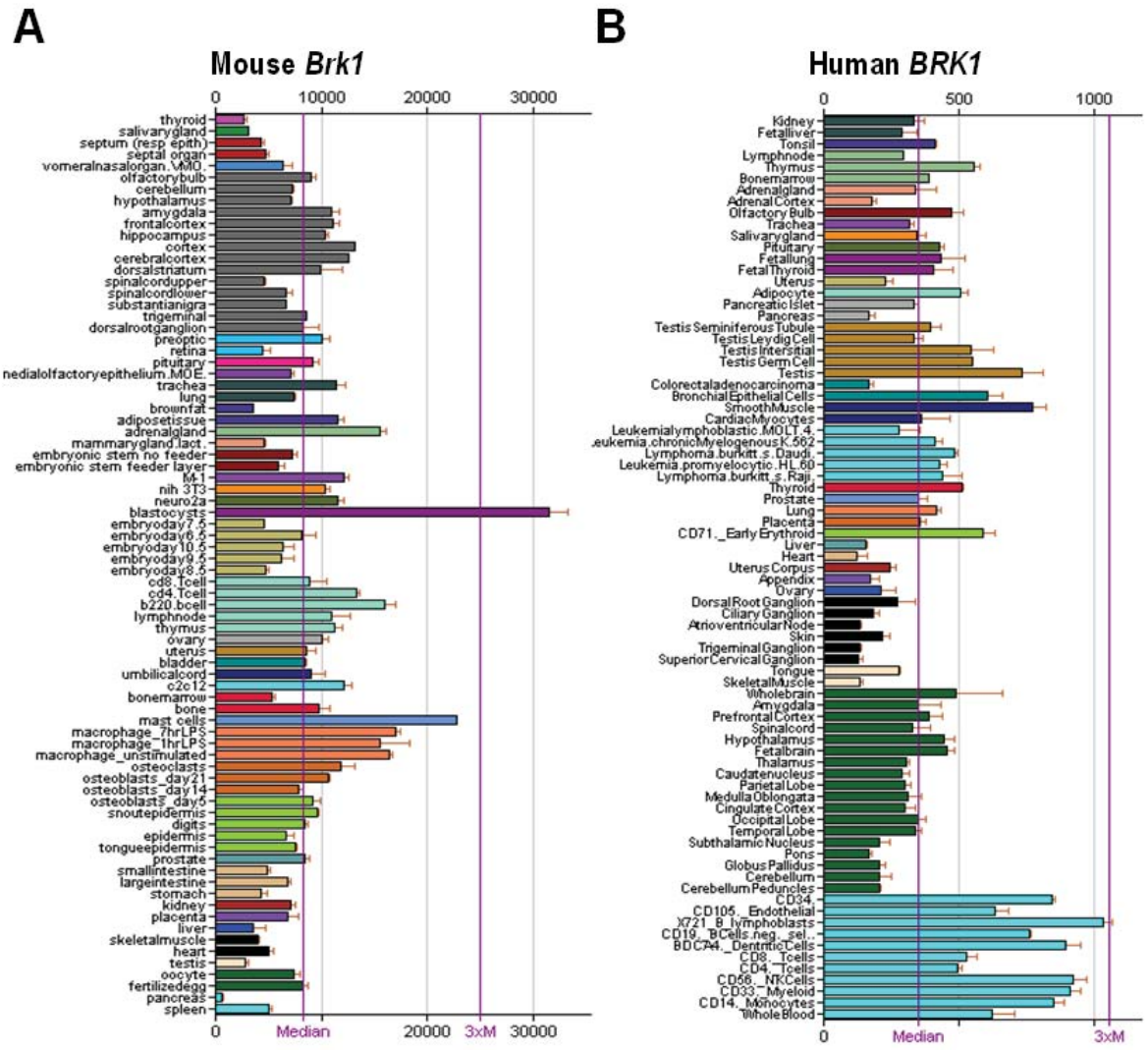

Escobar et al. Suppl. Figure 8